

**Optical evidence of multiphase coexistence in single crystalline (La,Pr,Ca)MnO<sub>3</sub>**

H. J. Lee, K. H. Kim,\* M. W. Kim, and T. W. Noh

*School of Physics and Research Center for Oxide Electronics, Seoul National University, Seoul 151-747, Korea*

B. G. Kim, T. Y. Koo, and S.-W. Cheong

*Department of Physics and Astronomy, Rutgers University, Piscataway, New Jersey 08854*

Y. J. Wang and X. Wei

*National High Magnetic Field Laboratory, Florida State University, Tallahassee, Florida 32310*

(Received 9 May 2001; revised manuscript received 18 October 2001; published 8 March 2002)

We investigated temperature ( $T$ )- and magnetic field-dependent optical conductivity spectra  $\sigma(\omega)$  of a  $\text{La}_{5/8-y}\text{Pr}_y\text{Ca}_{3/8}\text{MnO}_3$  ( $y \approx 0.35$ ) single crystal, showing intriguing phase coexistence at low  $T$ . At  $T_C < T < T_{CO}$ , a dominant charge-ordered phase produces a large optical gap energy of  $\sim 0.4$  eV. At  $T < T_C$ , at least two absorption bands newly emerge below 0.4 eV. Analyses of  $\sigma(\omega)$  indicate that the bands should be attributed to a ferromagnetic metallic phase and a charge-disordered phase that coexist with the charge-ordered phase. This optical study clearly shows that  $\text{La}_{5/8-y}\text{Pr}_y\text{Ca}_{3/8}\text{MnO}_3$  ( $y \approx 0.35$ ) is composed of multiphases that might have different lattice strains.

DOI: 10.1103/PhysRevB.65.115118

PACS number(s): 75.30.Vn, 71.30.+h, 78.20.Ci

**I. INTRODUCTION**

Recently, electronic phase separation in manganites has been the subject of various theoretical<sup>1,2</sup> and experimental<sup>3-8</sup> studies. Computational studies predicted that a strong tendency toward electronic phase separation in manganites could lead to an inhomogeneous ground state with hole-rich and hole-poor regions.<sup>1</sup> Indeed, many experimental tools probed evidence of mixed phases with various length and time scales in the wide phase space of manganites that was obtained by tuning of chemical pressure<sup>3-6</sup> and/or carrier (or impurity) doping.<sup>6-8</sup>

$\text{La}_{5/8-y}\text{Pr}_y\text{Ca}_{3/8}\text{MnO}_3$  revealed a unique type of phase separation into submicrometer-sized mixtures of ferromagnetic (FM) metallic and charge-ordered (CO) insulating domains.<sup>3</sup> With variation of  $y$ , the chemical pressure was varied to tune the volume fraction and the domain size of each component. It was found that the metal-insulator transition in the compound occurs through a percolation process, and that magnetoresistance can be dramatically enhanced due to the two-phase coexistence.

In spite of such interesting phenomena, the physical origin of the phase separation in  $\text{La}_{5/8-y}\text{Pr}_y\text{Ca}_{3/8}\text{MnO}_3$  is not yet fully understood. A hole segregation-type phase separation<sup>9</sup> was ruled out because the penalty in electrostatic energy was too large for the large-scale charge separation of submicrometer-sized domains.<sup>2,3</sup> Instead, Littlewood suggested that structural inhomogeneities should exist due to a large strain mismatch of the FM metallic and CO insulating domains.<sup>2</sup> Related to this suggestion, a neutron-scattering study by Radaelli *et al.* showed that a phase separation with the mesoscopic length scale (500–2000 Å) occurring in  $\text{Pr}_{0.7}\text{Ca}_{0.3}\text{MnO}_3$  could be driven by intragranular strain.<sup>10</sup> On the other hand, through an x-ray scattering study, Kiryukhin *et al.* indicated that an additional insulating phase might be present in a  $\text{La}_{5/8-y}\text{Pr}_y\text{Ca}_{3/8}\text{MnO}_3$  crystal as a function of temperature ( $T$ ).<sup>11</sup>

Up to this point, there have been a limited number of optical studies on phase separation behavior in manganites. Liu, Cooper, and Cheong<sup>12</sup> observed two absorption bands in optical conductivity spectra  $\sigma(\omega)$  of  $\text{Bi}_{1-x}\text{Ca}_x\text{MnO}_3$  at  $T_N < T < T_{CO}$ , that could be attributed to  $\sim 100$  Å scale mixtures of FM metallic and CO insulating domains. Jung *et al.*<sup>13</sup> also observed two infrared-absorption bands in  $\sigma(\omega)$  of  $\text{La}_{1/8}\text{Sr}_{7/8}\text{MnO}_3$  that suggested a phase separation between two FM phases which were orbital-ordered insulating and orbital-disordered metallic phases. These studies addressed the coexistence of two kinds of phases based on two absorption bands in  $\sigma(\omega)$ . However, there has been no report showing evidence of multiphase coexistence through optical conductivity studies of manganites.

In this paper, we present temperature ( $T$ )- and magnetic field ( $H$ )-dependent  $\sigma(\omega)$  of a  $\text{La}_{5/8-y}\text{Pr}_y\text{Ca}_{3/8}\text{MnO}_3$  ( $y \approx 0.35$ ) (LPCMO) single crystal. At  $T_C < T < T_{CO}$ , the CO phase shows a large optical gap energy of  $\sim 0.4$  eV, which remains finite above  $T_{CO}$ . At  $T < T_C$ , at least two additional absorption bands newly emerge below 0.4 eV. The absorption bands can be attributed to a FM metallic and a charge-disordered phase, appearing in the backbone of the charge-ordered phase below  $T_C$ . The  $T$ -dependent changes in the phonon spectra suggest that these multiphases have different degrees of lattice strain in each phase. The  $H$ -dependent  $\sigma(\omega)$  indicate that, with increasing  $H$  at 4.2 K, these coexisting multiphases become unified and eventually turn into a homogeneous FM metallic phase at 12 T.

**II. EXPERIMENTS AND RESULTS****A. Transport and magnetic properties**

A single crystal of LPCMO was grown by the floating-zone method using a mirror furnace. The sample was characterized by resistivity  $\rho$  and magnetization measurements using the four-probe method and a superconducting quantum interference device magnetometer, respectively. Figure 1(a)

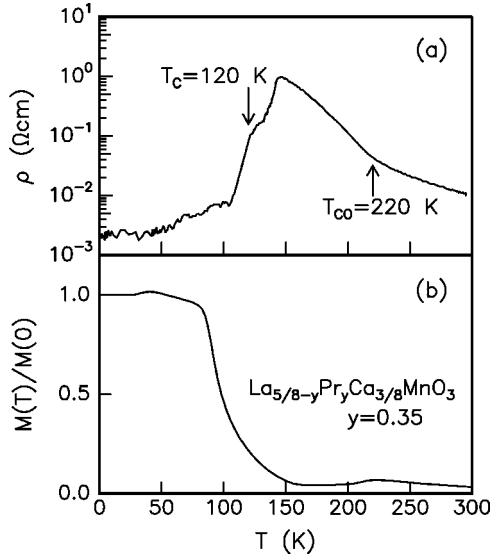


FIG. 1. (a)  $T$ -dependent resistivity  $\rho$  at zero magnetic field for a  $\text{La}_{5/8-y}\text{Pr}_y\text{Ca}_{3/8}\text{MnO}_3$  ( $y=0.35$ ) single crystal. (b)  $T$ -dependent normalized magnetization.

shows  $T$ -dependent  $\rho$  data for the LPCMO. With decreasing  $T$ , this sample undergoes a charge-ordering transition at  $T_{\text{CO}} \approx 220$  K, and then a relatively sharp insulator-metal transition around  $T_{\text{C}} \approx 120$  K. Near  $T_{\text{C}}$ , we can observe the steplike changes of  $\rho$  in the metal-insulator transition region. (Even for samples obtained from the same batch, the temperature where the steplike structures appear varies.) Similar steplike behaviors were observed not in LPCMO polycrystals but in single crystals,<sup>14</sup> which was attributed to the larger size of the FM domains in the single crystals. Below  $T_{\text{C}}$ , the  $\rho$  data show some fluctuations, which seem to be related to the reported random telegraph noise of LPCMO.<sup>15</sup> Therefore, our  $\rho$  response at low  $T$  suggests the coexistence of FM metallic and CO insulating domains with a temporal fluctuation. Figure 1(b) shows the normalized magnetization value,  $M(T)/M(0)$ , of the LPCMO crystal.  $M(T)/M(0)$  increases gradually around  $T_{\text{C}}$ , which is distinguished with the behavior of the FM transition in a homogeneous system. Also, the value of  $M(T)/M(0)$  saturates at low temperature where the FM state becomes dominant.

### B. $T$ dependence of optical spectra

We measured reflectivity spectra  $R(\omega)$  with various values of  $T$ . Detailed techniques for the  $R(\omega)$  measurements were described in our previous report.<sup>16</sup> Figure 2 shows  $T$ -dependent  $R(\omega)$  of the LPCMO single crystal. There are sharp structures due to transverse optic-phonon modes in the far-infrared region. As  $T$  approaches 150 K from 300 K,  $R(\omega)$  below 0.5 eV decreases, which is consistent with the dc resistivity behavior shown in Fig. 1(a). As  $T$  decreases further below  $T_{\text{C}}$ ,  $R(\omega)$  shows drastic increases, approaching the metallic response at 10 K.

Using the Kramers-Kronig (KK) relation, we obtained  $\sigma(\omega)$  from the measured  $R(\omega)$ .<sup>16</sup> Figure 3(a) shows  $T$ -dependent  $\sigma(\omega)$  above  $T_{\text{C}}$ . As  $T$  is lowered from 300 K,

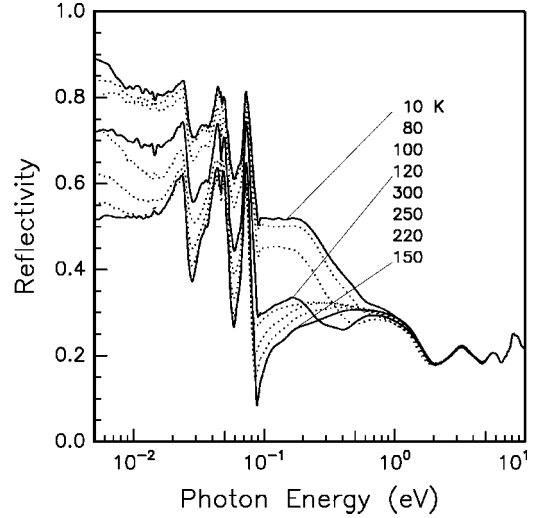


FIG. 2. (a)  $T$ -dependent  $R(\omega)$  of a  $\text{La}_{5/8-y}\text{Pr}_y\text{Ca}_{3/8}\text{MnO}_3$  ( $y=0.35$ ) single crystal.

$\sigma(\omega)$  below 0.5 eV is systematically suppressed and an optical gap clearly developed. With decreasing  $T$  and crossing  $T_{\text{CO}}$ , the peak position of the absorption band near 1.3 eV moves to a higher energy around 1.4 eV. This behavior illustrates that the charge ordering evolves as a consequence of the freezing out of charge and lattice, and eventually makes a clean charge gap larger, in accord with the more insulating nature of the CO state. Therefore, it is likely that the CO phase is dominant at  $T_{\text{C}} < T < T_{\text{CO}}$ , and that the broad band around 1.4 eV can be attributed to the characteristic optical response of the CO domains.

Figure 3(b) shows that, below  $T_{\text{C}}$ , absorption bands appear in the low-energy region. The features below  $\sim 0.5$  eV grow in strength as  $T$  decreases. Note that there is no Drude-

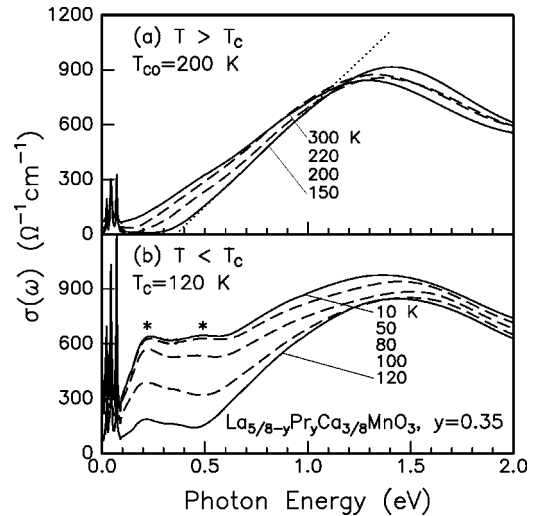


FIG. 3.  $T$ -dependent  $\sigma(\omega)$  (a) above and (b) below  $T_{\text{C}}$ . At  $T_{\text{C}} < T$ , the optical gap energy due to the CO phase is determined by drawing a linearly extrapolated line (dotted) at the inflection point of  $\sigma(\omega)$ . At  $T \leq T_{\text{C}}$ , at least two absorption bands appear in the midinfrared region. The peak positions of the bands are indicated as asterisks.

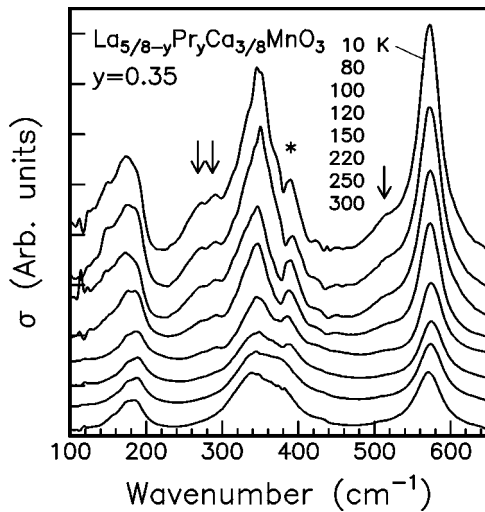


FIG. 4. Optic-phonon modes of  $\text{La}_{5/8-y}\text{Pr}_y\text{Ca}_{3/8}\text{MnO}_3$  ( $y=0.35$ ). Arrows indicate the additional phonon modes appearing below  $T_{\text{CO}}$ .

like peak even at the metallic state. As indicated by the asterisks,  $\sigma(\omega)$  at 10 K show at least two mid-IR absorption bands centered around 0.22 and 0.49 eV. As  $T$  decreases, the former remains located nearly at the same frequency, while the latter shifts to a higher frequency from 0.35 eV at 120 K to 0.49 eV at 10 K. This suggests that the origin of the lower-frequency peak might be different from that of the higher-frequency one. Even at  $T \ll T_{\text{C}}$ , the strength of a broad absorption band around 1.4 eV does not decrease. This is in contrast with the  $\sigma(\omega)$  behaviors of homogeneous FM metallic samples that show a significant spectral weight transfer from above 1.0 to below 1.0 eV.<sup>17</sup> [A similar spectral weight change was observed by applying  $H$ , which will be shown in Sec. II C.] This suggests that the volume fraction of the CO phase does not change significantly below  $T_{\text{C}}$ .

The evidence of the CO phase below  $T_{\text{C}}$  can also be seen in the  $T$ -dependent phonon spectra, shown in Fig. 4. Depending on the types of collective motions in perovskite materials, the phonons around 182, 346, and 572  $\text{cm}^{-1}$  are known as external, bending, and stretching modes, respectively.<sup>18</sup> Each phonon mode reflects the motion of related ions: The external mode represents the vibrating motion of the La (Pr or Ca) ions against the  $\text{MnO}_6$  octahedra. The bending mode is strongly affected by a change in the Mn-O-Mn bond angle. The stretching mode is sensitive to the Mn-O bond length. As shown in Fig. 4, the bending mode starts to be split near  $T_{\text{CO}}$ . A similar bending mode splitting was often observed when large anisotropic lattice distortions developed with the stabilization of charge ordering.<sup>19</sup> As  $T$  decreases below  $T_{\text{C}}$ , the additional bands around 270, 290, and 516  $\text{cm}^{-1}$  seem to grow continuously in intensity with the bending mode splitting. The persistence of the bending mode splitting below  $T_{\text{C}}$  indicates that the CO phase still remains in the low  $T$ .

### C. $H$ dependence of optical spectra

In order to further understanding, we performed melting experiments for the low-temperature CO phase by applying a

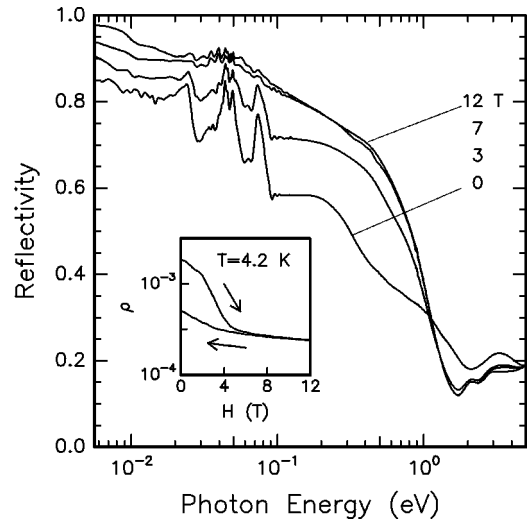


FIG. 5.  $H$ -dependent  $R(\omega)$  of  $\text{La}_{5/8-y}\text{Pr}_y\text{Ca}_{3/8}\text{MnO}_3$  ( $y=0.35$ ) single crystal at 4.2 K. Inset:  $H$ -dependent  $\rho$  measured at 4.2 K.

magnetic field. As shown in Fig. 5, the  $H$ -dependent  $R(\omega)$  were measured at a fixed  $T$  of 4.2 K using the facilities at National High Magnetic Field Laboratory at Tallahassee. Details of the  $H$ -dependent reflectivity measurements were described elsewhere.<sup>20</sup> With increasing  $H$ , the reflectivity increases and the phonon modes become screened. The inset of Fig. 5 shows the hysteresis of the  $\rho$  values measured at 4.2 K. With increasing  $H$ , the  $\rho$  value decreases abruptly at low  $H$  below 4 T, and nearly saturates above 4 T. With decreasing  $H$  from 12 to 0 T,  $\rho$  remains at a small value, not recovering to the original value at 0 T. This hysteresis can be explained by the fact that the CO phase melts into a FM phase in the field-increasing run, but the sample remains in the FM phase in the field-decreasing run. Similar metastable FM phases were reported in  $\text{Pr}_{0.69}\text{Ca}_{0.31}\text{MnO}_3$  and  $(\text{La}_{0.7}, \text{Nd}_{0.3})_{1.4}\text{Sr}_{1.6}\text{Mn}_2\text{O}_7$ .<sup>21</sup>

Figure 6 shows the  $H$ -dependent  $\sigma(\omega)$ , which were obtained from a KK analysis of  $R(\omega)$  in Fig. 5. With increasing  $H$ , the spectral weight above 1.0 eV becomes strongly suppressed and transferred to a low-frequency region. Although the sample shows a metallic resistivity at 3 T, the corresponding optical spectrum still has an asymmetric mid-IR band. At  $H=12$  T, a Drude-like peak can be clearly observed, and the absorption peak around 1.4 eV disappears.

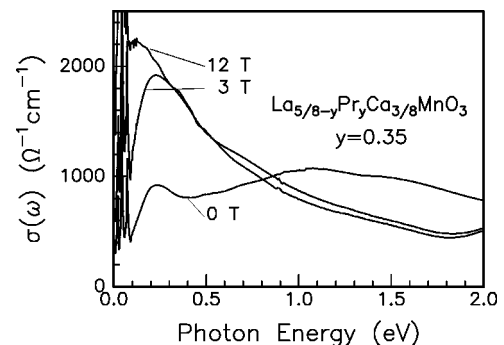


FIG. 6.  $H$ -dependent  $\sigma(\omega)$ .

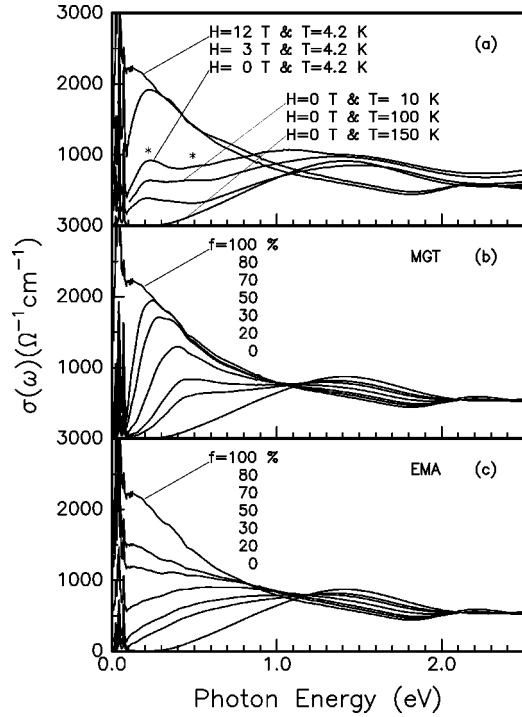


FIG. 7. (a)  $T$ - and  $H$ -dependent  $\sigma(\omega)$ . (b) The MGT and (c) the EMA predictions with various metal volume fractions  $f$ .

Strong asymmetric absorption bands below 1.4 eV were observed in the  $\sigma(\omega)$  of some homogeneous FM metallic manganites, and attributed to the large polaron absorption.<sup>17</sup> Note that the two absorption bands, shown in Fig. 3(b), are not observed in the data of Fig. 6 under high  $H$ . Therefore, it is evident that the optical spectra in Fig. 3(b) cannot be interpreted in terms of responses of a homogeneous FM metal.

### III. DISCUSSION

#### A. Failure of the two-phase description

One important question which we should address at this point is how we can interpret the low-frequency absorption features below  $T_C$ . In Fig. 7(a), we plot the  $T$ -dependent  $\sigma(\omega)$  at zero field and the  $H$ -dependent  $\sigma(\omega)$  together at fixed 4.2 K. Note that  $\sigma(\omega)$ , with  $H=0\text{ T}$  and  $T=150\text{ K}$ , represents the CO response, and the  $\sigma(\omega)$ , with  $H=12\text{ T}$  and  $T=4.2\text{ K}$ , represents the FM response. With decreasing  $T$  from 150 to 4.2 K, the spectral weight below 1 eV increases. Also, with increasing  $H$  at 4.2 K, a large spectral weight transfer occurs from above  $\sim 1\text{ eV}$  to below  $\sim 1\text{ eV}$ . Then, the simplest way to describe  $\sigma(\omega)$  below  $T_C$  is to use a two-phase description (that is, by assuming that each state is composed of the insulating CO and the metallic FM phases).

Optical properties of an inhomogeneous medium can be modeled by several effective-medium theories, which predict the effective optical conductivity  $\sigma_{eff}(\omega)$  in terms of  $\sigma(\omega)$  and the volume fraction of its constituent components. To check the validity of the two-phase description, we applied the two most commonly used effective-medium theories, i.e., the Maxwell-Garnet theory (MGT) and the Bruggeman-type

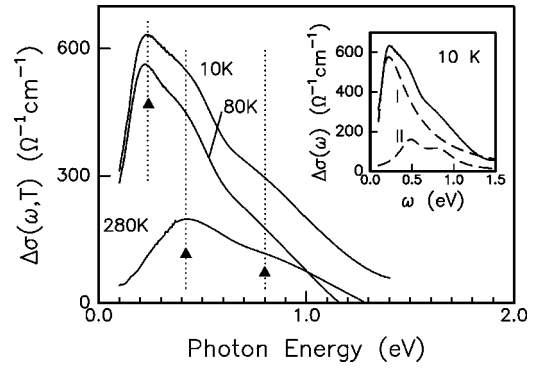


FIG. 8.  $\Delta\sigma(\omega, T) \equiv \sigma(\omega, T) - \sigma(\omega, 150\text{ K})$  for various temperatures. The  $\Delta\sigma(\omega, T)$  curves at  $T \leq T_C$  are composed of an asymmetric absorption band and small additional bands (filled triangles). The spectral shape of the additional bands are very similar to the shape of  $\Delta\sigma(\omega, T)$  at  $T \gg T_{CO}$ . The inset shows a  $\Delta\sigma(\omega, 10\text{ K})$  curve, and fitting results using an asymmetric line shape (for band I) and two Lorentzians (for band II).

effective-medium approximation (EMA). Details of these theories and their application to optical properties of composites can be found elsewhere.<sup>22</sup> Figures 7(b) and 7(c) show  $\sigma_{eff}(\omega)$  calculated using the MGT and EMA, respectively, for various values of  $f$ , which represent the volume fractions of the metallic domains. We used  $\sigma(\omega)$  at 150 K and at 12 T (and 4.2 K) as responses of the homogeneous insulating and metallic phases, respectively. It seems as though the MGT is more appropriate for describing the general features of the experimental data, shown in Fig. 7(a). However, none of the theories could reproduce the two peak structure below 0.5 eV, which was marked with the asterisks. This shows that a simple picture based on the two-phase description cannot explain the two absorption features observed below  $T_C$ .

#### B. Optical evidence of multiphase coexistence

To obtain further insight, we subtracted the optical response of the CO phases from the measured  $\sigma(\omega)$  at each temperature,  $\sigma(\omega, T)$ . It was assumed that  $\sigma(\omega, 150\text{ K})$  could represent the  $\sigma(\omega)$  of CO domains. Figure 8 shows the results for  $\Delta\sigma(\omega, T) \equiv \sigma(\omega, T) - \sigma(\omega, 150\text{ K})$  at various temperatures. The  $\Delta\sigma(\omega, 10\text{ K})$  curve is composed of an asymmetric absorption band peaked around 0.2 eV and a broad band with peaks around 0.4 and 0.8 eV. While the absorption band around 0.2 eV appears below  $T_C$ , the broad band with peaks around 0.4 and 0.8 eV already exists above  $T_{CO}$ .

To estimate these  $T$ -dependent spectral weight absorption bands quantitatively, we fitted  $\Delta\sigma(\omega, T)$  below  $T_C$  as a sum of an asymmetric band (band I) around 0.2 eV and two Lorentzians (band II) around 0.4 and 0.8 eV. The inset of Fig. 8 shows the  $\Delta\sigma(\omega, 10\text{ K})$  curve and its fitting results. It is found that band I is very similar to  $\sigma(\omega)$  at  $H=3\text{ T}$  in Fig. 6. Band II is very similar to  $\Delta\sigma(\omega, 280\text{ K})$  in Fig. 8. These observations strongly suggest that band I at low  $T$  should be associated with the FM metallic phase, and that band II should be attributed to another phase. The physical proper-

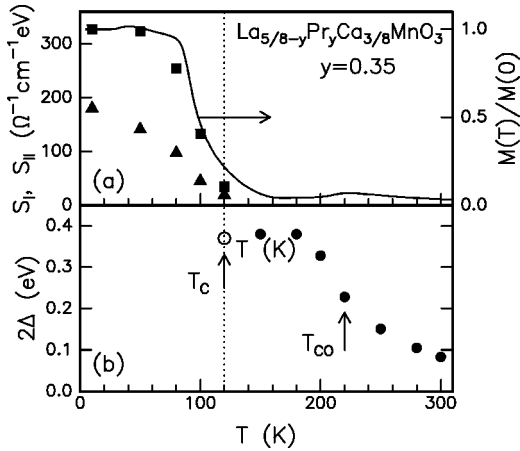


FIG. 9. (a)  $T$  dependence of the spectral weights  $S_I$  (solid squares) and  $S_{II}$  (solid triangles) at  $T \leq T_C$ . See inset of Fig. 4 and the texts for definitions. The solid line represents a normalized magnetization curve. (b)  $T$  dependence of the optical gap energy  $2\Delta$  (solid circles). The open circle represents  $2\Delta$  at  $T_C$ .

ties of this additional phase can be very similar to those of the high  $T$  charge-disordered (CDO) insulating phase.

Based on these analyses, we estimated the strengths of band I,  $S_I$ , and band II,  $S_{II}$ , below  $T_C$ . It is interesting to compare the  $T$  dependence of  $S_I$  and  $S_{II}$  with the normalized magnetization value,  $M(T)/M(0)$ . Figure 9(a) shows the  $T$  dependences of  $S_I$  (solid squares),  $S_{II}$  (solid triangles), and  $M(T)/M(0)$ . The observation that  $S_I$  is proportional to  $M(T)/M(0)$  indicates that band I is a result of FM spin ordering. Also, the smooth behavior of  $M(T)/M(0)$  is not consistent with the FM transition in a homogeneous system. Therefore,  $S_I$  can be attributed to the spectral weight of FM metallic domains in an inhomogeneous system. On the other hand,  $S_{II}$  increases with  $M(T)/M(0)$  near  $T_C$ , and it continuously increases even when  $M(T)/M(0)$  is saturated. This again confirms the above conclusion that band II is due to the absorption of a CDO insulating phase appearing additionally with the development of the FM phase below  $T_C$ . *All of these experimental findings suggest that there exist at least three phases, namely the FM metallic phase, the CO insulating phase, and the CDO insulating phase in LPCMO.*

### C. A possible origin of the charge-disordered phase

The existence of the CDO phase in LPCMO might be closely related to the strain developments suggested by Littlewood.<sup>2</sup> In perovskite manganites with strong Jahn-Teller (JT) electron-phonon interaction, anisotropic lattice strain can be developed by the JT distortion. In the CO state, it is well known that the anisotropic strain is quite large due to a cooperative JT distortion and a  $d_{z^2}$  orbital ordering. On the other hand, in a nearly homogeneous FM metallic state, the JT distortion becomes small. As  $T$  decreases below  $T_C$ , the FM phase starts to grow. If a single FM crystallite nucleates into a CO phase, it will be under a large stress from the surrounding CO crystals that discourages further growth. Then domains in different parts of the LPCMO crystal will form with the strain field in random orientations, so the in-

homogeneous strain cannot be easily released, leading to phase separation with a sub- $\mu\text{m}$  length scale. This can explain the dominance of the CO phases far below  $T_C$  and the hysteretic behavior of  $\rho$ , shown in the inset of Fig. 5. Moreover, due to a large strain mismatch between the FM and the CO phases, the interfacial region will have inhomogeneous strain and form the CDO phase.

The temperature dependence of the phonon spectra, shown in Fig. 4, also supports the suggested scenario based on the strain developments. It is well known that phonon modes are quite sensitive to local lattice distortions. Figure 4 shows that, with decreasing  $T$ , a phonon mode splitting around  $346 \text{ cm}^{-1}$  starts to occur near  $T_{CO}$  and remains even at  $T < T_C$ , in agreement with the dominance of the CO phase at the low temperature. Moreover, a few additional phonon structures, which are marked with arrows, clearly appear below  $T_{CO}$ , consistent with the existence of another phase (i.e., the CDO phase).

The asymmetric line shape of band I is indicative of the fact that the lattice distortion of the FM domains is not large.<sup>23</sup> On the other hand,  $\sigma(\omega)$  of the CO domains with large strains showed a band centered  $\sim 1.4 \text{ eV}$  with a large  $2\Delta \approx 0.4 \text{ eV}$ . Most of the spectral weights of band II appear in an energy region of 0.3–1.0 eV. This indicates that the lattice strain of the CDO region can be larger than that of the FM metallic domains, but smaller than that of the CO domains. According to our results in Figs. 3(b) and 8(a), the lower center frequency of band II and  $S_{II}$  increased as  $T$  decreased below  $T_C$ . This seems to indicate that the volume fraction, as well as the strain of the CDO domains, possibly located at the interface of FM and CO domains, increase with decreasing  $T$ . Therefore, our  $\sigma(\omega)$  data suggest that the lattice strains and their interplay with  $T$  among the three phases play a crucial role in determining the electronic and magnetic properties of the LPCMO.

### D. Charge-ordering gap of the CE-type CO phase

It is worthwhile to acquire quantitative information about the optical gap energy  $2\Delta$  at  $T_C \leq T$ . We drew a linear tangential line at the inflection point of  $\sigma(\omega)$ , and assigned its crossing energy with the abscissa as the gap value, shown as a dotted line in Fig. 3(a). Figure 9(b) shows the  $2\Delta$  vs  $T$  plot.  $2\Delta$  just above  $T_C$  is found to be as large as 0.38 eV. The value remains nearly the same for  $T_C \leq T \leq 180 \text{ K}$  and decreases slightly near  $T_{CO}$ . It should be noted that  $2\Delta \approx 0.38 \text{ eV}$  at  $T \approx 150 \text{ K}$  is comparable to the observed value of  $\text{La}_{1/2}\text{Ca}_{1/2}\text{MnO}_3$  [i.e.,  $2\Delta(0) \approx 0.45 \text{ eV}$  at the ground state].<sup>24</sup> Since the charge-ordering in LPCMO is known to be of the  $\text{La}_{1/2}\text{Ca}_{1/2}\text{MnO}_3$ -type, i.e., the so-called CE-type,<sup>3</sup> the large value of  $2\Delta$  of LPCMO can be ascribed to the characteristics of the CE-type CO phase.

It is also interesting to note that  $2\Delta \approx 0.22 \text{ eV}$  at  $T_{CO}$  and  $2\Delta \approx 0.1 \text{ eV}$  at 300 K. In other words,  $2\Delta$  does not become zero at  $T$  far above  $T_{CO}$ . This is in contrast with the behavior of many CO materials that show a nearly zero value of  $2\Delta$  at  $T_{CO}$ . These anomalous  $2\Delta$  behaviors indicate that there exist enhanced spatial and/or temporal fluctuations in the CO correlation far above  $T_{CO}$  in LPCMO.<sup>24</sup> The enhanced CO fluctu-

tuations can be a generic feature of LPCMO that has mixed phases near the phase boundary where a phase separation occurs as  $T \rightarrow 0$ .<sup>25</sup>

#### IV. SUMMARY

In conclusion,  $T$ - and  $H$ -dependent optical conductivity spectra of a  $\text{La}_{5/8-y}\text{Pr}_y\text{Ca}_{3/8}\text{MnO}_3$  single crystal revealed that, at  $T < T_C$ , at least two absorption bands emerge below 0.4 eV. The absorption bands can be attributed to a FM metallic phase and a charge-disordered phase that coexist with the charge-ordered phase. We also found that the LPCMO has a rather large charge gap, and shows a fluctuation in charge-ordered correlation above  $T_C$ . In addition, the  $T$ -dependent changes of the phonon modes as well as polaron bands suggest that the coexisting multiphase might have different lattice strains. Our  $\sigma(\omega)$  study supports that structural

as well as electronic phase separations occur in the LPCMO below  $T_C$ .

#### ACKNOWLEDGMENTS

We are grateful to H. K. Lee, Dr. J. H. Jung, Y. S. Lee, D. S. Suh, and Dr. Y. Chung for useful discussions and helpful experiments. This work was supported by the Ministry of Science and Technology through the Creative Research Initiative Program and by the Ministry of Education through the BK 21 Program. B.G.K., T.Y.K., and S.W.C. were partially supported by Grant Nos. NSF-DMR-9802513 and NSF-DMR-00-80008. Part of this work was performed at the National High Magnetic Field Laboratory, which is supported by the NSF Cooperative Agreement No. DMR-0084173 and by the State of Florida.

\*Present address: NHMFL, ES E536, Los Alamos National Laboratory, Los Alamos, NM 87545.

<sup>1</sup>See for a review, A. Moreo, S. Yunoki, and E. Dagotto, *Science* **283**, 2034 (1999); E. Dagotto, T. Hotta, and A. Moreo, *Phys. Rep.* **344**, 1 (2001).

<sup>2</sup>P.B. Littlewood, *Nature (London)* **399**, 529 (1999).

<sup>3</sup>M. Uehara, S. Mori, C.H. Chen, and S.-W. Cheong, *Nature (London)* **399**, 510 (1999).

<sup>4</sup>K.H. Kim, M. Uehara, C. Hess, P.A. Sharma, and S.-W. Cheong, *Phys. Rev. Lett.* **84**, 2961 (2000).

<sup>5</sup>N.A. Babushkina, A.N. Taldenkov, L.M. Belova, E.A. Chistotina, O.Yu. Gorbenko, A.R. Kaul, K.I. Kugel, and D.I. Khomskii, *Phys. Rev. B* **62**, R6081 (2000).

<sup>6</sup>Y. Moritomo, *Phys. Rev. B* **60**, 10 374 (1999).

<sup>7</sup>G. Allodi, R. De Renzi, G. Guidi, F. Licci, and M.W. Pieper, *Phys. Rev. B* **56**, 6036 (1997).

<sup>8</sup>T. Kimura, Y. Tomioka, R. Kumai, Y. Okimoto, and Y. Tokura, *Phys. Rev. Lett.* **83**, 3940 (1999).

<sup>9</sup>J.B. Goodenough and J.-S. Zhou, *Nature (London)* **386**, 229 (1997).

<sup>10</sup>P.G. Radaelli, R.M. Ibberson, D.N. Argyriou, H. Casalta, K.H. Andersen, S.-W. Cheong, and J.F. Mitchell, *Phys. Rev. B* **63**, 172419 (2001).

<sup>11</sup>V. Kiryukhin, B.G. Kim, V. Podzorov, S.-W. Cheong, T.Y. Koo, J.P. Hill, I. Moon, and Y.H. Jeong, *Phys. Rev. B* **63**, 024420 (2001).

<sup>12</sup>H.L. Liu, S.L. Cooper, and S.-W. Cheong, *Phys. Rev. Lett.* **81**, 4684 (1998).

<sup>13</sup>J.H. Jung, K.H. Kim, H.J. Lee, J.S. Ahn, N.J. Hur, T.W. Noh, M.S. Kim, and J.-G. Park, *Phys. Rev. B* **59**, 3793 (1999).

<sup>14</sup>V. Podzorov, M. Uehara, M.E. Gershenson, T.Y. Koo, and S.-W. Cheong, *Phys. Rev. B* **61**, R3784 (2000).

<sup>15</sup>B. Raquet, A. Anane, S. Wirth, P. Xiong, and S. von Molnar, *Phys. Rev. Lett.* **84**, 4485 (2000).

<sup>16</sup>H.J. Lee, J.H. Jung, Y.S. Lee, J.S. Ahn, T.W. Noh, K.H. Kim, and S.-W. Cheong, *Phys. Rev. B* **60**, 5251 (1999).

<sup>17</sup>K.H. Kim, J.H. Jung, and T.W. Noh, *Phys. Rev. Lett.* **81**, 1517 (1998); M. Quijada, J. Cerne, J.R. Simpson, H.D. Drew, K.H.

Ahn, A.J. Millis, R. Shreekala, R. Ramesh, M. Rajeswari, and T. Venkatesan, *Phys. Rev. B* **58**, 16 093 (1998); Y. Okimoto, T. Katsufuji, T. Ishikawa, T. Arima, and Y. Tokura, *ibid.* **55**, 4206 (1997).

<sup>18</sup>K.H. Kim, J.Y. Gu, H.S. Choi, G.W. Park, and T.W. Noh, *Phys. Rev. Lett.* **77**, 1877 (1996).

<sup>19</sup>T. Katsufuji, T. Tanabe, T. Ishikawa, Y. Fukuda, T. Arima, and Y. Tokura, *Phys. Rev. B* **54**, 14 230 (1996).

<sup>20</sup>J.H. Jung, H.J. Lee, T.W. Noh, E.J. Choi, Y. Moritomo, Y.J. Wang, and X. Wei, *Phys. Rev. B* **62**, 481 (2000).

<sup>21</sup>H.J. Lee, J.H. Jung, K.H. Kim, M.W. Kim, T.W. Noh, Y. Moritomo, Y.J. Wang, and X. Wei, *Physica C* **364–365**, 614 (2001); Y. Moritomo and M. Itoh, *Phys. Rev. B* **59**, 8789 (1999).

<sup>22</sup>T.W. Noh, Y. Song, S.-I. Lee, J.R. Gaines, H.D. Park, and E.R. Kreidler, *Phys. Rev. B* **33**, 3793 (1986).

<sup>23</sup>As a result of the strong electron-phonon coupling in manganites, the presence of a polaron absorption band is another important spectral feature of  $\sigma(\omega)$ . It is likely that the structural multiphase coexistence can also be understood based on this polaron picture. According to the polaron absorption theory [ D. Emin, *Phys. Rev.* **48**, 13 691 (1993); A.S. Alexandrov and A.M. Bratkovsky, *J. Appl. Phys.* **87**, 5016 (2000)], the peak energy of the incoherent band is roughly proportional to the binding energy of a polaron that increases as the local lattice distortion increases. In FM metallic manganites well below  $T_C$ , the mid-IR polaron band becomes quite asymmetric, and is centered below  $\sim 0.3$  eV, which is close to the line shape of incoherent absorption of a large polaron [ K.H. Kim, J.H. Jung, and T.W. Noh, *Phys. Rev. Lett.* **81**, 1517 (1998); D. Emin, *Phys. Rev.* **48**, 13 691 (1993).] Above  $T_C$ , as local JT lattice distortions increase, the band becomes rather symmetric, and the center frequency shifts to a higher frequency. This polaron band can be described as a small polaron absorption band.

<sup>24</sup>H.J. Lee, K.H. Kim, J.H. Jung, T.W. Noh, R. Suryanarayanan, G. Dhalenne, and A. Revcolevschi, *Phys. Rev. B* **62**, 11320 (2000); K.H. Kim, S. Lee, T.W. Noh, and S.-W. Cheong (unpublished).

<sup>25</sup>A. Moreo, S. Yunoki, and E. Dagotto, *Phys. Rev. Lett.* **83**, 2773 (1999).